Bioresource Technology 443 (2026) 133851

Contents lists available at ScienceDirect

Bioresource Technology

journal homepage: www.elsevier.com/locate/biortech

Aureobasidium pullulans NRRL 62042 as robust platform for efficient lignin valorization and sustainable *cis,cis*-muconic acid production☆

Marielle Driller [a,c], Marius Grad [b], Marie R.E. Dielentheis-Frenken [c], Karla Stein [a,c], Michael Kohlstedt [b], Christoph Wittmann [b], Lars M. Blank [a,d], Till Tiso [c,*]

[a] iAMB - Institute of Applied Microbiology. ABBt - Aachen Biology and Biotechnology, RWTH Aachen University, Worringerweg 1, D-52074 Aachen, Germany
[b] Institute of Systems Biotechnology, Saarland University, Campus A1.5, D-66123 Saarbrücken, Germany
[c] Systems Biotechnology, Faculty of Technology, Bielefeld University, Universitätsstr. 25, D-33615 Bielefeld, Germany
[d] WSS Research Centre "catalaix", Worringerweg 2, D-52074 Aachen, Germany

HIGHLIGHTS

- High tolerance of *Aureobasidium pullulans* towards various lignin-derived monomers.
- Growth on complex depolymerized lignins highlights strain robustness.
- 23 g L^{-1} muconic acid with complete catechol conversion in fed-batch fermentation.
- Fully sustainable process using lignin hydrolysate and hemicellulose-derived xylose.

GRAPHICAL ABSTRACT

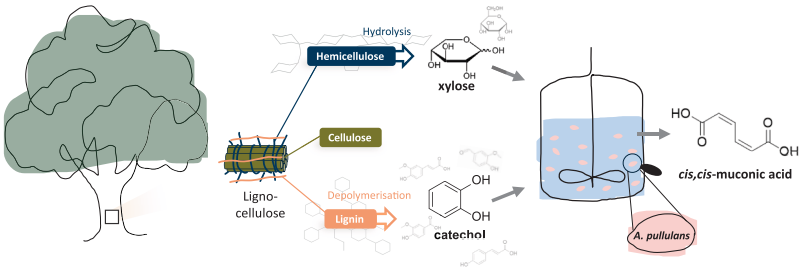

ARTICLE INFO

Keywords:
Aromatic monomers
Catechol
Xylose
Biorefinery
Platform chemical
Metabolic engineering

ABSTRACT

Lignin is a highly abundant source of renewable aromatics, but efficient microbial conversion remains challenging due to the limited substrate tolerance of many microorganisms. In this study, the polyextremotolerant yeast-like fungus *Aureobasidium pullulans* NRRL 62042 was identified as a robust host capable of growing on a range of lignin-derived monomers as well as on complex depolymerized lignins. One aromatic monomer generated during lignin depolymerization is catechol, which can be converted into the higher-value product muconic acid (MA) in a single enzymatic step. To channel catechol toward MA, a muconate cycloisomerase I deletion mutant was generated and evaluated in small-scale cultivations. MA production was further enhanced through the implementation of improved feeding strategies. Finally, fed-batch fermentation in a 1.2 L bioreactor showed efficient catechol conversion and production of 23 g L^{-1} MA. These findings position *A. pullulans* as a strong platform organism for sustainable lignin valorization and MA production.

Abbreviations: BCD, base-catalyzed depolymerization; C/N, carbon-to-nitrogen; CatA, catechol 1,2-dioxygenase; CatB, muconate cycloisomerase I; CDW, cell dry weight; DO, dissolved oxygen; G, coniferyl alcohol; H, *p*-coumaryl alcohol; HTC, hydrothermal conversion; MA, muconic acid; MM, minimal medium; OTR, oxygen transfer rate; OXD, oxidative depolymerization; PCA, protocatechuic acid; S, sinapyl alcohol; STY, space time yield; TE, trace element.

☆ This article is part of a special issue entitled: 'Lignin Valorization' published in Bioresource Technology.

* Corresponding author at: Systems Biotechnology, Faculty of Technology, Bielefeld University, Universitätsstr. 25, D-33615 Bielefeld, Germany.
E-mail addresses: marielle.driller@rwth-aachen.de (M. Driller), marius.grad@uni-saarland.de (M. Grad), marie.dielentheis-frenken@uni-bielefeld.de (M.R.E. Dielentheis-Frenken), karla.stein@rwth-aachen.de (K. Stein), michael.kohlstedt@uni-saarland.de (M. Kohlstedt), christoph.wittmann@uni-saarland.de (C. Wittmann), lars.blank@rwth-aachen.de (L.M. Blank), till.tiso@uni-bielefeld.de (T. Tiso).

https://doi.org/10.1016/j.biortech.2025.133851
Received 30 October 2025; Received in revised form 12 December 2025; Accepted 19 December 2025
Available online 21 December 2025

1. Introduction

Most everyday products — from fuels and chemicals to plastics and medicine — rely on limited fossil resources, and their production causes environmental stress and health risks (Wolf et al., 2025). Hence, there is a growing interest in developing sustainable production systems using low-cost, non-food bio-based resources (Wagh et al., 2024). Here, lignocellulose stands out due to its high abundance as a key structural element in plant cell walls. One of the three main components of lignocellulose is lignin, alongside cellulose and hemicellulose. Lignin is primarily composed of three types of monolignols: *p*-coumaryl alcohol (H), coniferyl alcohol (G), and sinapyl alcohol (S), which can be linked in several ways by ether and carbon–carbon bonds, resulting in a complex and heterogeneous three-dimensional structure (Abdelaziz et al., 2016). The structural complexity presents a major challenge for its valorization, leaving it largely underutilized (Beckham et al., 2016). Technical lignin, referring to lignin isolated from lignocellulosic biomass, is primarily obtained as a by-product of lignocellulosic processing industries, particularly the paper and pulp sector, which generates approximately 100 Mt/y of kraft lignin obtained from the kraft pulping process (Dessbesell et al., 2020). Currently, most technical lignin is burned for heat and energy production. To unlock lignin's full potential, strategies have emerged to valorize its complex aromatic structure by converting it into valuable platform chemicals, materials, and biofuels. One such approach involves the depolymerization of lignin into various aromatic compounds such as *p*-coumaric acid, vanillic acid, catechol, and others *via* thermal or chemical depolymerization (Van den Bosch et al., 2018). These aromatics can then serve as substrates for the production of diverse high-value biochemicals (Becker and Wittmann, 2019). Among these, muconic acid (MA) stands out as a particularly promising product. The unsaturated dicarboxylic acid exists in three isomeric forms (Fig. 1): *cis,cis*, *cis,trans*, and *trans,trans*. Naturally, *cis,cis*-MA is the only isomer produced, but depending on the pH value (pH < 7) and/or with the addition of heat, it spontaneously isomerizes into the *cis,trans* configuration (Carraher et al., 2017). It is a suitable monomer for polymerization and serves as a direct precursor for numerous derivatives with applications in the fine chemical, food, and polymer industries (Fig. 1) (Blaga et al., 2023). The most prominent products derived from MA are adipic acid, used for nylon-6,6, plasticizers and lubricants, and terephthalic acid, a precursor to produce polyethylene terephthalate for plastic containers and packaging (Khalil et al., 2020).

Biological production of MA could successfully be demonstrated with different metabolically engineered hosts, using pure aromatics (*e.g.,* catechol, benzoate), depolymerized lignin containing complex aromatic mixtures, or carbohydrates such as glucose and glycerol (Choi et al., 2020; Rosini et al., 2023). The highest production so far was achieved with *Corynebacterium glutamicum,* with a titer of 85 g L^{-1} from catechol (Becker et al., 2018) and 88 g L^{-1} MA from glucose (Li et al., 2024). The only eukaryotic production host so far has been an engineered

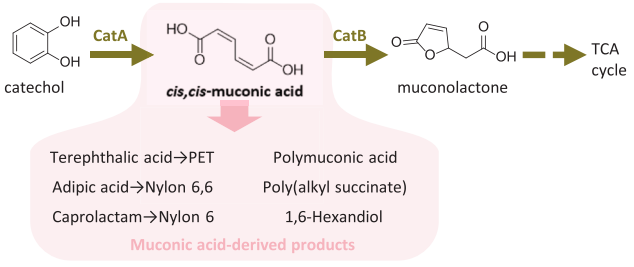

Fig. 1. Conversion of catechol into *cis,cis*-muconic acid and potential muconic acid-derived products. The green arrows show the metabolic pathway for catechol conversion into *cis,cis*-muconic acid in *Aureobasidium pullulans* NRRL 62042, which is then converted into muconolactone and, *via* various steps, funneled into the tricarboxylic acid (TCA) cycle. CatA: Catechol 1,2-dioxygenase, CatB: muconate cycloisomerase I.

Saccharomyces cerevisiae strain with a maximum titer of 22.5 g L^{-1} MA by *de novo* synthesis from glucose (G. Wang et al., 2022). Using eukaryotic production hosts has various advantages since they show high tolerance to low pH values, higher resistance towards toxic compounds, and the ability to use alternative carbon sources like xylose or hemicellulose (Patra et al., 2021).

A promising alternative eukaryotic host for biotechnological application is the polyextremotolerant yeast-like fungus *Aureobasidium.* This genus displays remarkable adaptability, tolerating extreme pH values, low temperatures, and high osmolarities. In contrast to common model organisms such as *Escherichia coli*, which require mild, nutrient-rich conditions that favor contamination by other microorganisms, *Aureobasidium* can grow efficiently under harsh environments, reducing both contamination risk and sterilization demands (Chen and Wan, 2017; Xiao et al., 2024). Moreover, the fungus shows a broad substrate spectrum, including agricultural side streams such as hemicellulose hydrolysate or potato waste, and produces various biotechnologically interesting compounds, such as pullulan, polymalic acid, and biosurfactants (P. Wang et al., 2022; Wani et al., 2021). It has already been reported that *Aureobasidium* sp. can grow on monomers that derive from lignin degradation, like benzoic acid, *p*-hydroxybenzoic acid, ferulic acid, vanillin, protocatechuic acid (PCA), and catechol (Bourbonnais and Paice, 1987). Altogether, the remarkable robustness, which manifests itself in a high tolerance to extreme conditions, and diverse product spectrum make *Aureobasidium* a promising host for application in an economically improved biotechnology.

In the first part of this study, the versatility and adaptability of *Aureobasidium pullulans* NRRL 62042 (hereafter referred to as *A. pullulans*) were investigated, and its ability to utilize a range of lignin-derived aromatics, even under varying pH conditions, was demonstrated. Furthermore, the strain demonstrated growth on different lignin depolymerization products containing complex mixtures of these aromatics.

In the second part of the study, we focused on MA production. Inspired by the observed metabolization of catechol, an aromatic intermediate generated during lignin depolymerization, a muconate cycloisomerase I (*CATB)* deletion mutant for MA production from catechol was engineered. MA production was initially established in microtiter plate cultivation. Subsequently, a co-feeding strategy with glucose and catechol was implemented in shake flask experiments to enhance MA titers. To improve sustainability, glucose was replaced with xylose, a non-food lignocellulosic sugar. Finally, process scalability of MA production was validated in 1.2 L bioreactors.

2. Materials and methods

2.1. Strains, media and culture conditions

For cloning and plasmid propagation, *Escherichia coli* pir2 was used. Strains were cultured in LB liquid medium (10 g L^{-1} peptone, 10 g L^{-1} sodium chloride, 5 g L^{-1} yeast extract) or on LB agar plates with 20 g L^{-1} agar added. 100 μg mL^{-1} ampicillin was added as a selection marker for plasmid maintenance.

The wildtype strain *A. pullulans* NRRL 62042 was provided by the USDA-ARS Culture collection (NRRL). For MA production, *A. pullulans* Δ*catB* was used. Strains were grown on YPD agar plates (20 g L^{-1} peptone, 10 g L^{-1} yeast extract, 20 g L^{-1} glucose, 20 g L^{-1} agar). For the growth test on different lignin-derived monomers and toxicity tests, a minimal medium (MM) (1 g L^{-1} K_2HPO_4, 0.8 g L^{-1} $MgSO_4$, 1 g L^{-1} NaCl, 1 mL L^{-1} vitamin solution, 10 mL L^{-1} trace element (TE) solution) developed by Haala et al. (2024) was used. NH_4NO_3 was added to start at a carbon-to-nitrogen (C/N) ratio of 25 g_{carbon} per $g_{nitrogen}$. The vitamin solution was composed of (per liter): 0.05 g D-biotin, 1 g D-calcium pantothenate, 1 g nicotinic acid, 25 g myo-inositol, 1 g thiamine hydrochloride, 1 g pyridoxine hydrochloride, and 0.2 g *para*-aminobenzoic acid and TE solution contained per liter: 1.5 g EDTA, 0.45 g $ZnSO_4{\cdot}7H_2O$, 0.10 g $MnCl_2{\cdot}4H_2O$,

0.03 g $CoCl_2 \cdot 6H_2O$, 0.03 g $CuSO_4 \cdot 5H_2O$, 0.04 g $Na_2MoO_4 \cdot 2H_2O$, 0.45 g $CaCl_2 \cdot 2H_2O$, 0.3 g $FeSO_4 \cdot 7H_2O$, 0.10 g H_3BO_3, and 0.01 g KI. For MA production and growth on lignin monomer mixtures, an adapted version of the optimized MLP medium from Haala et al. (2024) was used, which is referred to below as optimized MM. The C/N ratio was adjusted to 10 g_{carbon} per $g_{nitrogen}$ and the concentrations of the media components were enhanced as follows. For 25 g L^{-1} glucose, 1.89 g L^{-1} K_2HPO_4, 0.38 g L^{-1} $MgSO_4$, 0.38 g L^{-1} NaCl, 1.9 g L^{-1} NH_4NO_3, 0.38 mL L^{-1} vitamin solution, 3 mL L^{-1} TE solution were used. The medium components were adjusted in relation to the amount of glucose or xylose used. All cultivations of *A. pullulans* were performed at 30 °C.

2.2. Plasmid and strain construction

Knockout of the 1,125 bp *CATB* gene was performed by homologous recombination with 1,000 bp homologous flanking regions. The flanking regions were amplified from gDNA from *A. pullulans* with primers MD208/MD277 and MD276/MD211 with overhangs for Gibson assembly. The sequences of all primers used can be found in supplementary table 1. The *CATB* gene was replaced with a nourseothricin resistance cassette, driven by a phosphoglycerate kinase I promoter and terminated with a polyadenylation signal, flanked by LoxP sites to allow for potential excision *via* Cre-recombinase-mediated recombination (Zhang et al., 2019). For the characterization of the *CATB* knockout strain, excision of the resistance marker was not performed. Initially, the 26S-rDNA-loxp-P_{PGK}-NAT-polyA-loxp-P_{TEF}-18S-rDNA sequence from the plasmid pAMEXlox-1 (Zhang et al., 2019) was synthesized and cloned into the standard vector pMA-RQ (AmpR; ThermoFisher Scientific, Waltham, USA), yielding plasmid pAPloxp1. Then, the loxp-P_{PGK}-NAT-polyA-loxp cassette was amplified from pAPloxp1 with MD278/MD279. The pJET1.2 plasmid with an ampicillin resistance and ColE1 ori served as the backbone and was amplified using primers MDF-84 and MDF-83. All PCRs were performed with Q5 High-Fidelity DNA Polymerase (New England BioLabs, Ipswich, MA, USA). Plasmid assembly was performed using NEBuilder HiFi DNA Assembly Master Mix (New England BioLabs, Ipswich, MA, USA) and confirmed by colony PCR with OneTaq Quick-Load 2X MM w/Std Buffer (New England BioLabs, Ipswich, MA, USA) and Sanger sequencing (Eurofins Genomics, Ebersberg, Germany). The repair fragment was amplified from the assembled plasmid with MD212/MD213 and used for transformation of *A. pullulans* protoplasts. The protoplast formation and transformation procedure can be found in the supplementary data. Successful knockout of *CATB* was confirmed by colony PCR using the 2x Phire Plant Direct PCR Master Mix (Thermo Scientific, Waltham, MA, USA) and cell lysates of the respective colonies. To obtain the cell lysate, a colony was picked and resuspended in 100 µL of 5 % Chelex (w/v) and approximately 200 µL volume of 0.5 mm ceramic beads, followed by vortexing for 15 min and incubation at 100 °C for 5 min.

2.3. Toxicity of aromatic monomers and growth on monomers

To determine the growth-inhibitory concentration of different aromatic compounds that derive from the degradation of lignin and to investigate growth on respective lignin monomers as a sole carbon source, *A.pullulans* was cultivated in 24-well plates with 1.5 mL culture volume and shaking at 250 rpm and 30 °C in the Growth Profiler 960 (EnzyScreen BV, Heemstede, Netherlands). Growth was monitored by measuring the green value as a proxy for biomass. A green value-based growth rate was calculated for internal comparison, but this metric is not directly comparable to OD-based growth rates. In these experiments, commercially available chemicals were used as model compounds representative of the lignin-derived aromatics. The precultures were performed in MM medium with 10 g L^{-1} glucose in 100 mL shake flask with 10 % filling volume and shaking at 300 rpm. For the toxicity test, the main culture was inoculated to an OD_{600} of 0.3 with the same medium used for the preculture, with 10 g L^{-1} glucose and different concentrations of the respective aromatic monomers. For PCA, *p*-coumaric acid, 4-hydroxybenzoic acid, benzoic acid, ferulic acid, and vanillic acid growth with 5, 10, 20, 60, and 80 mM was tested. For vanillin, catechol, syringic acid, and phenol, presumed to be more toxic, growth with 5, 10, 20, 40, and 50 mM was evaluated. When no growth was observed after 60 h of cultivation, the respective concentration of lignin-derived monomer was considered as the growth-inhibitory concentration. To investigate growth on the respective lignin-derived monomers as the sole carbon source and to analyze the effect of pH on growth, another Growth Profiler cultivation was performed with the same preculture as described before. To avoid transferring glucose to the main culture, the cells were washed with 0.9 % NaCl before inoculation of the main culture. The concentration of the tested aromatic compounds was 5 mM, and the start pH of the medium was adjusted with 2 M NaOH or 2 M HCl to pH 4, 6, and 8. When no growth was observed after 60 h of cultivation, it was considered no growth. Experiments were performed in duplicates.

2.4. Depolymerization of lignin

Softwood kraft lignin (IndulinAT, Ingevity Corp., North Charleston, SC, USA), as well as wheat-straw organosolv lignin (Biolignin, Compagnie Industrielle de la Matière Végétale, Labège, France) were depolymerized in a 500 mL stainless steel stirred pressure vessel (Type 4575A, Parr Instruments, Moline, IL, USA) using either hydrothermal conversion (HTC) (Kohlstedt et al., 2018), oxidative depolymerization (OXD) (Abdelaziz et al., 2016) or base-catalyzed depolymerization (BCD) (Rodriguez et al., 2017).

For HTC, 7.5 g of IndulinAT softwood lignin was suspended in 250 mL demineralized water, loaded into the reactor vessel, and purged three times with nitrogen under stirring at 400 rpm. Depolymerization was carried out at 395 °C and 312 bar, achieving sub- and supercritical water conditions. After a reaction time of 60 min, the reactor content was rapidly quenched in an ice bath.

For OXD, an amount of 3 g of IndulinAT softwood lignin was suspended in 150 mL of a 0.2 M sodium hydroxide solution. The reaction mixture was flushed with pure oxygen by purging three times while stirring at 400 rpm and pressurized with 3 bar O_2. The reaction was carried out for 1 h at 160 °C and was instantly stopped by applying an ice bath.

BCD of straw lignin (Biolignin) was carried out by suspending 7.5 g lignin in 250 mL 0.5 M sodium hydroxide solution, purging three times with nitrogen under stirring at 400 rpm, and subsequently heating up to 120 °C and holding for 30 min (Weiland et al., 2025).

For cultivation purposes, HTC and OXD liquors were further concentrated *via* vacuum evaporation (2.5 h, 15 mbar, 40 °C, Christ RVC 2–33 IR, Martin Christ GmbH, Osterode, Germany). All depolymerized lignins were neutralized and freed from solid residues by centrifugation (5,000 x *g*, 5 min, room temperature) followed by filtration (0.45 µm). Aromatic monomer composition was quantified by high-performance liquid chromatography (HPLC) and confirmed by Gas chromatography-mass spectrometry as described previously (Barton et al., 2018; Weiland et al., 2025). Monomeric yields and aromatic compositions are given in supplementary table 2.

2.5. Online monitoring of growth on depolymerized lignin fractions

Cultivations with lignin-derived fractions were carried out using a µTOM device (Adolf Kühner AG, Birsfelden, Switzerland) to monitor the oxygen transfer rate (OTR) in 24-well plates. Further information on the use of OTR data and its comparison with optical growth measurement is provided in Ladner et al. (2016). The precultures were grown for 20 h in optimized MM containing 25 g L^{-1} glucose in a 100 mL shake flask with 10 % filling volume. To evaluate the growth of *A. pullulans* on processed lignin fractions, cultures were prepared with a total volume of 2 mL, using either 5 % (v/v) HTC catechol-rich hydrolysate, 6.6 % (v/v) OXD

vanillin-rich depolymerization product, or 45 % (v/v) and 70 % (v/v) of the BCD *p*-coumaric acid-rich liquor as the sole carbon source. All other media components were used in a concentration that corresponds to 10 g L^{-1} glucose.

2.6. Production of cis,cis-muconic acid in 24-well plates

The strain *A. pullulans* Δ*catB* was used for MA production from catechol (Thermo Fisher Scientific, Waltham, USA) and catechol-rich hydrolysate. The preculture was done as described in chapter 2.5 with 25 g L^{-1} glucose or xylose. The main culture was performed in 24-well Growth Profiler plates for 62 h and 250 rpm with optimized MM medium with 10 g L^{-1} glucose or xylose and 5 mM of catechol or 4 % (v/v) catechol-rich hydrolysate. To maintain a pH above 7 for stable production of *cis,cis*-MA and avoid conversion to *cis,trans*-MA below pH 7, 100 mM of MOPS buffer (pH 7.2) was added to the medium. For sampling, an entire well was harvested, and samples for HPLC measurement were prepared. Experiments were performed with biological triplicates.

2.7. Online monitored fed-batch cultivation in shake flasks

For a first fed-batch approach, the cultivation was done in a 500 mL unbaffled shake flask with 5 % filling volume and 300 rpm. The TOM shaker device (Adolf Kühner AG, Birsfelden, Switzerland) was used for online monitoring of the OTR which was calculated according to Anderlei et al. (2004). The main culture was inoculated to an OD_{600} of 0.5, and the initial batch phase was done in optimized MM with 10 g L^{-1} glucose and 100 mM MOPS buffer (pH 7.2). All media components were used in a concentration that corresponds to 25 g L^{-1} glucose. When the OTR decreased, 5 mM catechol and 10 g L^{-1} glucose were fed. This was repeated three times. Experiments were performed with biological duplicates.

2.8. Dissolved oxygen-based fed-batch in 1.2 L stirred tank bioreactors

Fermentation was performed in a 1.2 L glass bioreactor with the BioFlo120 fermentation system (Eppendorf, Hamburg, Germany) equipped with a Pt100 temperature sensor, dissolved oxygen (DO) probe (InPro6830, Mettler-Toledo, Columbus, Ohio, USA), and a pH probe (EASYFerm Plus PHI 225, Hamilton, Bonaduz, Switzerland). For off-gas analytics, BlueVary off-gas sensors (BlueSens gas sensor GmbH, Herten, Germany) were used. The bioprocess was controlled with the DASware Control Software (v 5.3.1.; Eppendorf, Hamburg, Germany). The preculture was prepared as described for cultivation in 24-well plates. For the main culture (V_0 = 500 mL) optimized MM was used, and the culture was inoculated to an OD_{600} of 0.5 and fermentation was started in batch-mode with 50 g L^{-1} (333 mM) xylose, with the DO controlled at 30 % by an agitation cascade. Air supplementation was done with 0.5 vvm (volume air per volume medium per minute). During batch-mode, the pH was kept constant at pH 6 with the addition of 2 M NaOH or 2 M H_2SO_4. After depletion of xylose, indicated by an increase of the DO, fermentation was switched to fed-batch mode. The agitation cascade was turned off, the agitation rate was set to 560 rpm, and the pH was adjusted to pH 7.5. The feeding phase was initiated with a manual feed of 10 mL feeding solution (250 g L^{-1} xylose, 250 mM catechol), which corresponds to 5 mM catechol and 5 g L^{-1} (33 mM) xylose in the fermenter. For further feeding steps, a script for automatic feeding (see supplementary data) was used, and the feed was started if the DO reached a value of 65; however, this trigger point was adjusted during the course of the fermentation. The feed rate was 120 mL h^{-1} with a feeding volume of 10 mL per feed shot. At a later stage of cultivation, nitrogen pulses were added to the cultivation medium to sustain cellular activity. Each pulse contained 10 % of the $NaNO_3$ initially supplied in the medium, resulting in 0.38 g L^{-1} per pulse.

2.9. High-performance liquid chromatography

Quantification of aromatic monomers, *cis,cis*-MA, *cis,trans*-MA, xylose, and glucose using HPLC is described in the supplementary data.

3. Results and discussion

3.1. A. pullulans is able to grow on diverse lignin-derived aromatic monomers

Given the increasing interest in lignin valorization, we first examined whether *A. pullulans* can utilize lignin-derived aromatic monomers as growth substrates (Fig. 2A). The strain *A. pullulans* NRRL 62042 has already been characterized as a good polyol lipid producer and is genetically accessible (Xiao et al., 2024), making it a promising candidate for future biotechnological applications involving aromatic compound valorization.

Many aromatics that derive from lignin degradation are weak phenolic acids whose undissociated forms are membrane-permeable and can disrupt cellular homeostasis, making them more toxic under acidic conditions (Ndukwe et al., 2020). Hence, growth was evaluated across a range of initial medium pH values (4, 6, and 8). For an additional toxicity test, the medium was supplemented with 10 g L^{-1} glucose and buffered to pH 6. Aromatic compounds were added at concentrations of up to 80 mM, and their inhibitory effects on growth were evaluated.

The results show that *A. pullulans* was able to utilize most of the tested aromatic monomers as sole carbon sources across all tested pH values, including both acidic and alkaline conditions (Fig. 2A). Detailed results for the growth and toxicity test, as well as the green value-based growth rates for the toxicity test, can be found in the supplementary data.

The fungus showed growth on the central aromatic degradation intermediates PCA and catechol, which are commonly produced *via* funneling pathways from upstream lignin-derived compounds (Weiland et al., 2022). Moreover, the strain exhibited notably high tolerance to PCA, indicating efficient channeling into the central carbon metabolism, potentially *via* the β-ketoadipate pathway. These results are supported by a previous genome mining study by Xiao et al. (2025), in which the genes encoding key enzymes such as catechol 1,2-dioxygenase and protocatechuate 3,4-dioxygenase were identified in *A. pullulans* NRRL 62031 (GeneBank assembly: GCA_023079325.1) – a strain with a high genomic similarity to *A. pullulans* NRRL 62042 (GeneBank assembly: GCA_036418965.1). These enzymes catalyze the aromatic ring cleavage of PCA and catechol *via* the *ortho*-cleavage pathway, and the resulting intermediates are funneled into the β-ketoadipate pathway. Remarkably, these dioxygenases are well-established biomarkers for microbial aromatic compound degradation in soil and wastewater environments, and their presence in *A. pullulans* provides the basis for potential applications in the bioremediation of aromatic pollutants (Nafian et al., 2016).

Among the H-type phenolic acids, *A. pullulans* grew well on both *p*-coumaric acid and 4-hydroxybenzoic acid (Fig. 2A). The toxicity test showed that the strain could still grow with monomer concentrations of up to 80 mM. For 4-hydroxybenzoic acid, the green value-based growth rate was almost the same for all tested concentrations, while for *p*-coumaric acid, the rate was significantly reduced at 60 mM and 80 mM, with a 42 % reduction at 80 mM compared to growth on glucose alone. However, these results indicate a high tolerance, especially toward 4-hydroxybenzoic acid, and a good tolerance toward *p*-coumaric acid. A similar trend was observed for *C. glutamicum*, which showed almost no decrease in growth rate with increasing concentrations of 4-hydroxybenzoic acid, whereas a stronger inhibitory effect was detected for *p*-coumaric acid (Weiland et al., 2023). For *Pseudomonas putida* KT2440 – a Gram-negative bacterium known for its ability to tolerate and metabolize diverse aromatic compounds (Jiménez et al., 2002) – the lethal concentration of *p*-coumaric acid was demonstrated to be 80 mM, a

A

	Lignin-derived monomers [5 mM]	Tested pH values pH 4	pH 6	pH 8	GIC** [mM]
Aromatic acids	Protocatechuic acid*	■	■	■	> 80
	Benzoic acid				20
G-type	Ferulic acid	■	■	■	80
	Vanillin			■	10
	Vanillic acid	■	■	■	> 80
Phenolics	Catechol*	■	■	■	10
	Phenol				10
	o-Cresol				10
H-type	*p*-Coumaric acid	■	■	■	> 80
	4-Hydroxybenzoic acid	■	■	■	> 80
S-type	Syringic acid	■			> 50

*key intermediate in degradation of aromatics
GIC: Growth-inhibitory concentration
■ = Growth
= No growth
**at pH 6

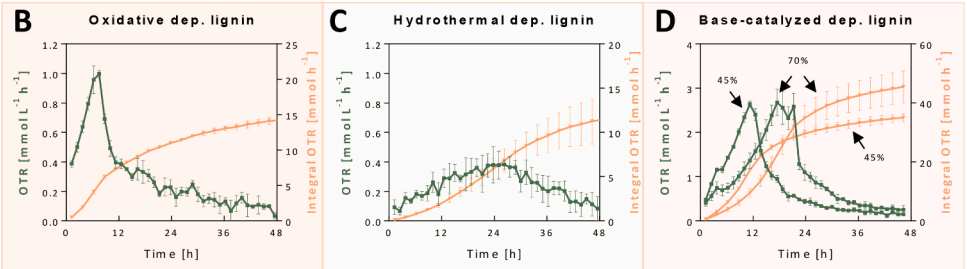

Substrate concentration	Amount [mM]
Vanillic acid	0.7
Vanillin	0.15
Acetovanillon	0.2

Substrate concentration	Amount [mM]
Catechol	1.7
4-Methylcatechol	0.36
3-Methylcatechol	0.22
4-Ethylcatechol	0.52

Substrate concentration	Amount [mM] with 70%
p-Coumaric acid	0.98
Ferulic acid	0.62
Vanillic acid	0.16

Fig. 2. Growth of *A. pullulans* NRRL 62042 on lignin-derived aromatic monomers and depolymerized lignins. A) Growth tests on lignin-derived monomers as sole carbon sources were performed in 96-well plates in minimal medium with 5 mM of respective monomers for 60 h. Growth-inhibitory concentration (GIC) was determined by adding different concentrations of the respective compound to minimal medium with 10 g L^{-1} glucose and 100 mM MES buffer (pH 6). The concentration at which no growth was observed after 60 h was considered as GIC. The data show mean values of duplicates with standard deviation. B, C, D) Cultivation of *A. pullulans* NRRL 62042 on depolymerized lignin fractions in μTOM with online monitoring of oxygen transfer rate (OTR). The cultivation was done in 24-well plates with 2 mL optimized minimal medium with 6.6 % (v/v) of oxidative-depolymerized lignin (B), 5 % (v/v) of hydrothermal-depolymerized lignin (C), and 45 % and 70 % (v/v) of base-catalyzed depolymerized lignin (D) at 30 °C and 300 rpm. The tables below show the initial aromatic composition in the cultivation medium. For aromatic compositions and monomeric yields of the prepared depolymerized lignins, see supplementary data. The data show mean values of triplicates with standard deviation.

concentration at which *A. pullulans* still exhibited growth (Salvachúa et al., 2018). This demonstrates the potential of *A. pullulans* to compete with already established bacterial platforms in terms of tolerance to H-type phenolic acids.

For the G-type aromatics, the most prominent representatives, ferulic acid, vanillin, and vanillic acid were tested (Fig. 2A) (Weiland et al., 2022). Vanillin is very reactive and exhibits a toxic effect on most microorganisms (Priefert et al., 2001). However, the growth on vanillin was possible at a pH of 8, and the growth-inhibitory concentration was 10 mM. For ferulic acid and vanillic acid, growth was observed at all tested pH values, and *A. pullulans* showed a high tolerance to the aromatics. In comparison, toxicity tests with *S. cerevisiae* demonstrated a complete inhibition of growth with the addition of 10.3 mM ferulic acid (Zhang et al., 2024) and 17.9 mM vanillic acid (Gu et al., 2019). By contrast, *A. pullulans* was still able to grow with 60 mM ferulic acid and 80 mM vanillic acid, underlining its high tolerance compared to other eukaryotic microorganisms like baker's yeast. Depending on the plant type and the process of lignin depolymerization, the composition of the monolignols in technical lignin varies. In the most common lignin production process, the kraft pulping process, the resulting technical lignin is mainly composed of G-type lignin (Becker and Wittmann, 2019). Therefore, the ability of *A. pullulans* to tolerate and metabolize G-type aromatics such as ferulic and vanillic acid highlights its promise for lignin valorization applications.

As a representative S-type lignin-derived compound, syringic acid was used to assess the growth capacity of *A. pullulans* (Fig. 2A). S-type units make up a large proportion of hardwood lignin (Becker and Wittmann, 2019); however, they are less commonly utilized by microorganisms, likely due to the structure of S-type lignin monomers with two methoxy groups, compared to a single or absent methoxy group in G- and H-type units, respectively (Abdelaziz et al., 2016). Nonetheless, demethylation of syringic acid has been reported for some fungi (Umashankar and Nygård, 2024) and for certain bacterial strains like *Sphingobium* sp. strain SYK-6 (Araki Takuma et al., 2020) or *Pseudomonas* sp. NGC7 (Ookawa et al., 2025). However, in a study by Ramírez-Morales et al. (2021), it was shown that all *Pseudomonas* strains (including KT2440) tested in their study did not grow on syringic acid. Interestingly, *A. pullulans* exhibited weak but observable growth on syringic acid at pH 4, and the toxicity assay revealed that it tolerated concentrations of up to 50 mM – the highest concentration tested.

In summary, the ability of *A. pullulans* to naturally metabolize all three lignin-derived H-, G-, and S-type monomers demonstrates its potential for valorizing heterogeneous lignin streams from lignocellulosic biomass, demonstrating a broad applicability in lignin-based biorefinery processes. Moreover, the fungus capacity to metabolize most of the compounds across a wide pH range highlights its robustness.

3.2. Depolymerized lignin as an alternative growth substrate for A. pullulans

Building on its solid growth on individual aromatics such as *p*-coumaric acid and catechol, we next investigated the ability of *A. pullulans* to grow on complex lignin depolymerization products obtained *via* different depolymerization methods. Three types of fractions were tested: (1) an OXD softwood lignin enriched in vanillic acid and vanillin; (2) a HTC hydrolysate containing mainly catechol and its alkylated derivatives as the predominant compounds; and (3) a wheat-straw-derived BCD liquor rich in *p*-coumaric acid, ferulic acid, and vanillic acid (Fig. 2B–D). Due to the brownish coloration of these fractions, growth experiments were conducted in a μTOM shaker system (Adolf Kühner AG, Birsfelden, Switzerland), which allowed for real-time monitoring of the OTR as a proxy for metabolic activity.

For the vanillic acid-rich OXD lignin fraction, a clear increase in OTR was observed, with a maximal OTR of 1 mmol $L^{-1}h^{-1}$ (Fig. 2B), indicating respiratory activity and efficient substrate utilization by the fungus. In contrast, the catechol-rich hydrolysate showed a lower OTR response, with a maximal OTR of 0.38 mmol $L^{-1}h^{-1}$, even though the substrate concentration was higher than in the OXD product (Fig. 2C). The highest OTR and integral OTR were observed with BCD wheat-straw lignin, with a maximal OTR of 2.6 mmol $L^{-1}h^{-1}$ with 45 % (v/v) and 2.7 mmol $L^{-1}h^{-1}$ with 70 % (v/v) liquor (Fig. 2D). Using 70 % (v/v) of the BCD liquor resulted in a prolonged lag phase compared to 45 % (v/v). HPLC analysis at the end of the cultivations revealed complete consumption of vanillic acid, vanillin, and acetovanillone in the culture with the OXD fraction. In addition, catechol and its alkylated derivatives were also fully depleted in the HTC hydrolysate. This hydrolysate additionally contained low concentrations of the potentially toxic aromatic compounds phenol and guaiacol, which were measured after hydrothermal depolymerization (see supplementary table 2), but not explicitly determined in the cultivation medium. For the cultivation with the BCD product, complete consumption of *p*-coumaric acid and ferulic acid was observed, while a small amount of vanillic acid (0.1 mM) remained in the cultivation medium. These results demonstrate the capability of *A. pullulans* to efficiently metabolize mixtures of aromatic compounds present in different depolymerized lignins. A hydrothermally depolymerized lignin containing mainly catechol has also been successfully used as a substrate for cultivations with *C. glutamicum* (Becker et al., 2018) and *P. putida* (Kohlstedt et al., 2018). In these studies, feed pulses containing sub-inhibitory catechol amounts were applied in fed-batch experiments to minimize catechol toxicity, as elevated concentrations can disrupt cellular metabolism and reduce overall fitness. Similarly, *A. pullulans* achieved complete catechol metabolization with a catechol concentration of 1.7 mM in the cultivation medium, indicating that it may be well suited for similar fed-batch processes with catechol-rich hydrolysates.

Since cultivation with OXD and BCD fractions resulted in rapid growth of *A. pullulans* with short lag phases, it can be expected that the monomeric concentration in the cultivation medium could be further increased. The toxicity test showed that *A. pullulans* was still able to grow with 5 mM vanillin, but with a prolonged lag phase. For *P. putida*, a lignosulfonate depolymerization product concentration resulting in 8 mM vanillin still supported good growth, demonstrating a higher tolerance of the bacterium toward this aromatic compound. However, the strain used was genetically engineered for improved vanillin metabolism (Bekirovska et al., 2025). In contrast, vanillic acid caused only a slight decrease in the green value-based growth rate, with 0.15 h^{-1} observed with 80 mM supplementation compared to 0.18 h^{-1} on glucose alone. A stronger inhibitory effect was observed for ferulic and *p*-coumaric acid, yet *A. pullulans* still grew with 60 mM ferulic and 80 mM *p*-coumaric acid, indicating that higher concentrations of the BCD straw lignin hydrolysate could be tolerated.

Unlike the HTC- and OXD-derived lignins, which were concentrated prior to cultivation, the BCD lignin liquor was used directly without prior concentration. Consequently, higher volume fractions of the BCD liquor (up to 70 % (v/v)) were added to the cultivation; however, this still resulted in comparatively low aromatic monomer concentrations of 0.98 mM *p*-coumaric acid, 0.62 mM ferulic acid, and 0.16 mM vanillic acid. Further preparatory steps, such as solvent extraction or the use of ionic liquids, may be required to further increase the concentration of aromatics, albeit at the expense of higher overall process costs. Although the aromatic concentrations in the BCD cultivation were comparatively low, rapid growth was observed, indicating low toxicity and suggesting the presence of additional growth substrates. HPLC analysis showed no residual sugars but did detect small amounts of acetic acid (up to 5 mM), which may also be metabolized by *A. pullulans*.

Regarding growth on BCD wheat straw lignin, comparable results were reported for *C. glutamicum*. The bacterium grew well on a complex BCD product containing 1.04 mM *p*-coumaric acid and 0.78 mM ferulic acid (Weiland et al., 2025).

Overall, these findings confirm the feasibility of using depolymerized lignin as a sustainable carbon source for *A. pullulans*. The utilization of all tested fractions provides compelling proof of principle for lignin valorization *via* microbial fermentation. While various lignocellulosic depolymerization fractions have previously been employed as substrates for *Aureobasidium* sp., particularly for the production of pullulan and polymalic acid (P. Wang et al., 2022), this study is, to the best of our knowledge, the first to demonstrate that *A. pullulans* can grow on depolymerization products purely from the lignin fraction, without any sugars derived from the hemicellulosic or cellulosic components. This finding nicely complements emerging strategies aimed specifically at developing lignin-standalone processes, further advancing the potential for sustainable biotechnological applications based solely on lignin. Future work should explore the fungus capacity to produce value-added compounds from lignin-based substrates.

3.3. Engineered strain A. pullulans NRRL 62042 ΔcatB efficiently converts catechol to cis,cis-muconic acid

After confirming that *A. pullulans* is capable of metabolizing catechol, we subsequently investigated its conversion to MA, as catechol can be transformed directly into MA in a single enzymatic step *via* the *ortho*-cleavage pathway (Khalil et al., 2020). Catechol is not only a relevant depolymerization product of lignin, such as from HTC-processed lignin (Kohlstedt et al., 2018), lignin pyrolysis, or lignin demethylation followed by catalytic hydrogenolysis (Kim et al., 2021), but also a central intermediate formed from various other lignin-derived monomers, like

p-coumaric acid, ferulic acid, and benzoic acid, when used for MA production (Choi et al., 2020). To enable MA accumulation, *CATB* (GenBank accession number: KAK6008233.1) was deleted (Fig. 1) *via* homologous recombination. The deletion was successful and resulted in stable integration of the gene deletion cassette, as confirmed by PCR (see supplementary figure 4). Upon cultivation with 10 g L^{-1} (56 mM) glucose and 5 mM catechol, the *ΔcatB* strain showed complete conversion of catechol to MA, resulting in a titer of 5 mM MA with no detectable side-product formation (Fig. 3A). Although the achieved titer of 5 mM was low, it provides a promising starting point for MA production with *A. pullulans*. Interestingly, it appeared that *A. pullulans ΔcatB* initially converted catechol into MA before utilizing glucose as a carbon source for growth (Fig. 3A). Catechol is a reactive aromatic compound known to exert cytotoxic effects (Schweigert et al., 2001). To mitigate cellular damage, the fungus may prioritize the conversion of catechol to MA, thereby neutralizing its toxic effects before it continues to grow on glucose. MA was detected in the cultivation medium, suggesting that the compound is efficiently exported to the extracellular environment, potentially reducing its cytotoxic effects and simultaneously simplifying the purification process. An approach to shorten the lag phase and to accelerate catechol conversion into MA could be enhanced expression of the catechol 1,2-dioxygenase (CatA), for example, by using strong synthetic promoters or additional copies of the gene, as it was shown for *P. putida* or *C. glutamicum* (Becker et al., 2018; Kohlstedt et al., 2018). This might increase the catechol conversion rate and could improve the tolerance of *A. pullulans* to catechol. Another approach could be to pre-induce *A. pullulans* cells with benzoic acid. It was shown in *P. putida* that cells pre-induced with benzoic acid exhibited a higher CatA activity and thus higher catechol conversion rates (Kohlstedt et al., 2018).

Moreover, the *CATB* deletion mutant was unable to grow on catechol as the sole carbon source (see supplementary figure 5), confirming the essential role of CatB in downstream catabolism and further supporting the *ortho*-cleavage pathway for catechol degradation.

In summary, the ability to efficiently accumulate MA from catechol highlights the strain's potential as a promising microbial platform for producing valuable biotechnological products using lignin-derived aromatics.

3.4. Optimization of cultivation conditions increases muconic acid titer

Initial batch cultivation using *A. pullulans ΔcatB* yielded a low MA titer of 5 mM, highlighting the need for process optimization to enhance product formation. However, catechol's inherent toxicity limits the feasibility of high initial concentrations, necessitating a controlled feeding strategy. To address this, a pulsed-feeding approach in 500 mL shake flasks was implemented using the TOM shaker system (Adolf Kühner AG, Birsfelden, Switzerland) to measure OTR. Briefly, 1.5 mL of feed solution containing glucose and catechol was added to the shake flask. The process began with a batch phase on glucose to support initial biomass formation. After 15 h, the supplied 10 g L^{-1} (56 mM) glucose was fully consumed. The initial biomass formation was followed by the sequential feeding of both glucose and catechol (indicated by asterisks, Fig. 3B), resulting in a concentration of 5 g L^{-1} (28 mM) glucose and 5 mM catechol in the medium. This co-feeding strategy was chosen based on prior observations that feeding catechol without supplementation with glucose led to its accumulation in the medium without efficient conversion to MA (see supplementary figure 5) as it was also demonstrated for *C. glutamicum* (Becker et al., 2018) and *P. putida* (Kohlstedt et al., 2018). This is likely due to limited metabolic activity in the absence of a readily utilizable carbon source. Monitoring the cell dry weight (CDW) revealed that the first glucose pulse supported additional biomass formation, whereas subsequent feed pulses did not result in further CDW increases. This indicates that the additional glucose was not used for growth but rather for sustaining cell viability and metabolic activity. Under these conditions, the fed catechol was efficiently converted into MA with a final titer of 15 mM after 67 h of cultivation and a 100 % conversion of catechol into MA. This confirms that pulsed feeding not only mitigates catechol toxicity but also sustains metabolic activity required for its conversion to MA. However, despite the improved production, a notable pH drop down to 4.5 occurred after 48 h of cultivation. The acidification led to partial isomerization of *cis,cis*-MA to *cis, trans*-MA in the later stages of cultivation, yielding a mixture of both

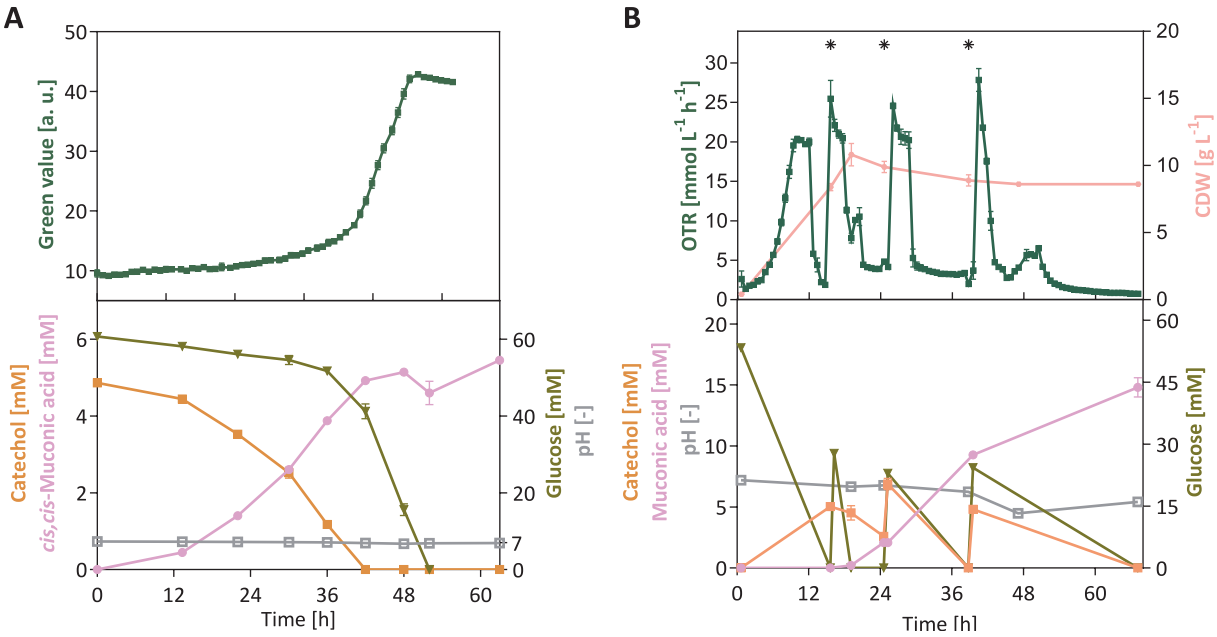

Fig. 3. Cultivation of *A. pullulans* NRRL 62042 Δ*catB* for muconic acid production. A) Batch cultivation in 24-deep-well Growth Profiler plates using optimized minimal medium with 10 g L^{-1} (56 mM) glucose and 5 mM of catechol at 30 °C, 250 rpm for 62 h. The data show mean values of triplicates with standard deviation. B) Fed-batch cultivation in shake flasks with an initial batch phase done in optimized minimal medium with 10 g L^{-1} glucose (56 mM). After consumption of glucose, the feeding phase started with three feeding events with 5 g L^{-1} (28 mM) glucose and 5 mM catechol each. The cultivation was done for 68 h at 30 °C and 300 rpm. Asterisks (*) indicate the feeding events. Produced muconic acid consists of both *cis,cis*- and *cis,trans*-isomers. The data show mean values of duplicates with standard deviation. CDW: cell dry weight.

isomers as confirmed by HPLC. The isomerization can lead to the formation of unwanted side products such as muconolactone, which can hinder downstream processing and complicate purification (Carraher et al., 2017; Khalil et al., 2020). Nevertheless, the observed 100 % conversion to MA suggests that no significant side-product formation occurred.

Taken together, with the employed feeding strategy, the MA titer was successfully increased threefold. Additionally, the importance of maintaining a stable pH throughout the process was emphasized. Future optimization should include active pH control or more efficient buffering strategies to preserve product stability and further improve MA titer.

3.5. Replacing glucose with the non-food sugar xylose enables more sustainable cis,cis-muconic acid synthesis

To improve bioprocess sustainability and move toward non-food carbon sources, glucose was replaced with xylose, a pentose sugar abundant in lignocellulosic biomass, with an extraction process that does not compete with food production. Thus, *A. pullulans ΔcatB* was cultivated with 5 mM catechol and 10 g L^{-1} (67 mM) xylose in 24-well plates using the Growth Profiler 960 (EnzyScreen BV, Heemstede, Netherlands). Complete conversion of catechol into MA was achieved, reaching a titer of 5 mM (Fig. 4A) – identical to the titer with glucose. This result clearly demonstrates that xylose can serve as a sufficient energy source to drive the conversion of catechol. Notably, the maximum growth rate on xylose (μ_{max} = 0.13 h^{-1}) was even slightly higher than on glucose (μ_{max} = 0.12 h^{-1}). The ability of *A. pullulans* to efficiently metabolize xylose sets it apart from many commonly used microbial hosts, such as *P. putida* and *C. glutamicum,* which typically require engineering to utilize xylose effectively (Gopinath et al., 2012; Meijnen et al., 2008). Additionally, the only eukaryotic organism used for MA production so far, *S. cerevisiae*, lacks the native ability to metabolize xylose. For the combined production of MA and ethanol from glucose, xylose, and catechol, several heterologous enzymes had to be integrated, including CatB for the conversion of catechol to MA and a xylose isomerase to ensure xylose metabolism (Liu et al., 2020). Overall, this result supports the feasibility of developing a fully lignocellulose-based production process for MA, utilizing both hemicellulosic sugars and lignin-derived aromatics.

3.6. Process intensification enables high-titer cis,cis-muconic acid production

Building on successful fed-batch cultivation in shake flasks and the cultivation using xylose as a sustainable carbon source, a bioreactor fed-batch fermentation approach with xylose and catechol was developed to further increase the MA titer (Fig. 4B). In this fed-batch setup (V_0 = 500 mL), an initial batch phase with 50 g L^{-1} (333 mM) xylose was used to build up biomass. The pH during the batch phase was set to 6, as this value was found to be beneficial for faster growth. After 24 h, once xylose was consumed, the pH was adjusted to 7.5 to stabilize production of *cis,cis*-MA. The feeding phase was initiated with a manual feeding pulse of 10 mL from a solution containing 250 mM catechol and 250 g L^{-1} xylose, which helped analyze the dissolved oxygen (DO) response. After a first strong DO decrease due to oxygen-dependent catechol conversion to MA, the DO increased, followed by a second decrease triggered by xylose consumption. A high DO peak was observed upon full xylose depletion. This pattern was then used to establish an automated DO-based feeding strategy: new pulses were triggered once the DO spike indicated full depletion of both substrates.

Importantly, catechol was fully consumed with no observable accumulation, and MA steadily accumulated over the cultivation period, resulting in a final titer of 162 mM (23 g L^{-1}) after 141 h (Fig. 4B). This represented a tenfold increase compared to the shake flask cultivation shown previously and corresponds to a space–time yield (STY) of 0.16 g $L^{-1}h^{-1}$. Stabilizing the pH at 7.5 proved effective, with HPLC analyses confirming that the majority of MA remained in the preferred

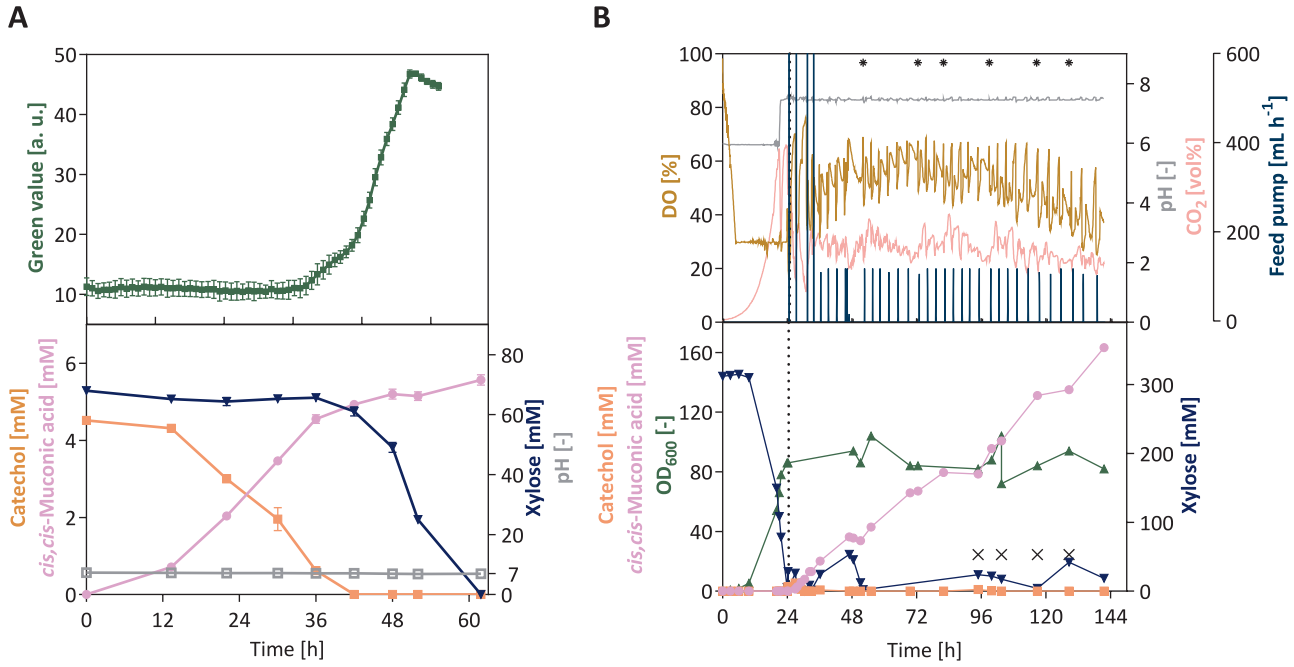

Fig. 4. Cultivation of *A. pullulans* NRRL 62042 Δ*catB* for *cis,cis*-muconic acid production with catechol and xylose. A) Batch cultivation in 24 deep-well Growth Profiler plates using optimized minimal medium with 10 g L^{-1} (67 mM) xylose and 5 mM of catechol at 30 °C, 250 rpm for 62 h. The data show mean values of triplicates with standard deviations. B) DO-based fed-batch fermentation with optimized MM with 50 g L^{-1} (333 mM) xylose in batch phase (V_0 = 500 mL, pH_{batch} 6, DO-control by varying stirrer rate from 200 to 1000, 30 °C). The vertical dotted line indicates the start of the feeding phase. The feeding solution contained 250 g L^{-1} (1.7 M) xylose and 250 mM catechol. 10 mL feed shots were given after an increase in DO, which signals catechol and xylose consumption. * indicate nitrogen pulses, × indicate culture broth removal at vessel limit (pH_{feed} = 7.5, stirrer rate set to 560 rpm, aeration with 100 % air and 0.5 vvm, n = 1).

cis,cis-isomeric form. To date, this is among the highest reported MA titers achieved with a eukaryotic host. For comparison, the closest titer achieved was 22.5 g L^{-1} in a heavily engineered *S. cerevisiae* strain synthesizing MA *de novo* from glucose. However, in a scale-up approach using a 10 L fermenter, a higher STY of 0.21 g L^{-1} h^{-1} was achieved (G. Wang et al., 2022).

During the fed-batch cultivation, a slowdown in the metabolization of both catechol and xylose was observed. This suggested a potential onset of cellular metabolic fatigue or nutrient limitation, which could impede the efficiency of MA production. To sustain cellular activity, nitrogen pulses were supplied to the bioreactor at regular intervals. Following the addition of nitrogen (as marked by an asterisk in Fig. 4B), faster substrate consumption was observed, as evidenced by a sharp decline in DO (see supplementary figure 6), indicating a revitalization of cellular metabolic activity. This underscores the importance of monitoring and adjusting nutrient levels in prolonged fermentations to maintain optimal bioconversion efficiency. The observed slowdown in catechol and xylose consumption may also result from toxic effects of accumulated MA. For *P. putida*, 60 g L^{-1} MA was shown to be the toxic concentration, while concentrations between 25 and 30 g L^{-1} resulted in a 30 % lower growth rate and a twofold extension of the lag phase (Salvachúa et al., 2018). Another organism used for MA production, *C. glutamicum,* remained viable at considerably higher concentrations, and an impressive titer of 85 g L^{-1} (598 mM) was achieved, demonstrating higher tolerance of this bacterium to MA. Interestingly, the intracellular MA concentration was very low, at 100 µM, indicating a highly active MA exporter that may play a key role in conferring this elevated tolerance (Becker et al., 2018). To gain deeper insights into MA production with *A. pullulans*, determining the inhibitory effects of MA is crucial for estimating the strain's maximal achievable titer.

In summary, the fed-batch fermentation using catechol and xylose as carbon sources demonstrates the scalability of MA production with *A. pullulans* Δ*catB* and confirms the fungus ability to achieve sustainable, high-yield MA production from non-food carbon sources.

3.7. Valorization of aromatic lignin hydrolysate for sustainable cis,cis-muconic acid production

To demonstrate the feasibility of lignin-derived fractions as feedstock for biotechnological production of MA, a proof-of-principle experiment was conducted using HTC catechol-rich hydrolysate. Due to a limited availability of the HTC catechol-rich hydrolysate, the experiment was carried out in the microtiter scale in 24-well plates using the Growth Profiler system (EnzyScreen BV, Heemstede, Netherlands). The Δ*catB* deletion strain, previously shown to accumulate MA from catechol, was cultivated with 4 % (v/v) HTC catechol-rich hydrolysate and 10 g L^{-1} (67 mM) xylose as a carbon source (Fig. 5). After a lag phase of 18 h, cell growth started. HPLC analysis revealed that catechol present in the hydrolysate was already efficiently converted to MA during the lag phase. Consistent with previous experiments, a complete catechol conversion was achieved, with 1.2 mM catechol converted to 1.2 mM MA. Interestingly, it was observed that not only catechol but also its methyl- and ethylated derivatives were metabolized by *A. pullulans,* and additional peaks in the HPLC chromatogram occurred, indicating the production of methyl- and ethylated MA variants. The peaks eluted later than MA, suggesting more hydrophobic compounds, consistent with what would be expected for the MA derivatives; however, no further analysis was performed. A similar promiscuity and substrate acceptance of CatA for methyl- and ethylated catechol derivatives and the conversion into methyl- and ethylated MA has previously been reported for *P. putida* and *Amycolatopsis* (Barton et al., 2018; Kohlstedt et al., 2018).

Moreover, it was tested whether variation in the co-substrate sugar would influence growth and MA production. For simplification, only xylose was used as a hemicellulose-derived C_5 sugar in this experiment; however, hemicellulose hydrolysis typically yields a mixture of C_5 and C_6 sugars (Huang et al., 2021). To verify that such a mixture of C_5 and C_6 sugars does not affect the MA production process, an additional cultivation was performed using the HTC hydrolysate combined with a mixture of xylose and glucose as substrate. The utilization of both sugars did not affect growth or MA production from catechol. The corresponding data are provided in supplementary figure 7.

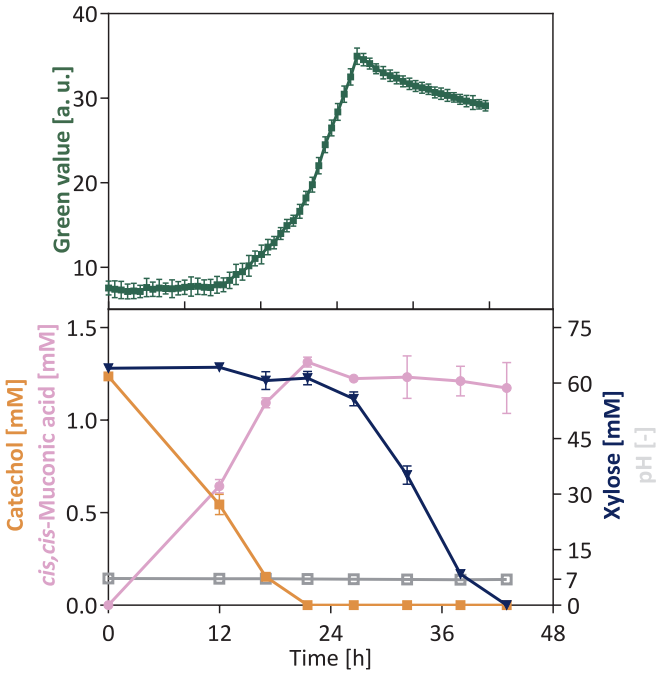

Fig. 5. Cultivation with *A. pullulans* NRRL 62042 Δ*catB* for *cis,cis*-muconic acid production from catechol-rich hydrolysate. Cultivation was carried out in 24 deep-well Growth Profiler plates in optimized minimal medium with 10 g L^{-1} (67 mM) xylose and 4 % (v/v) of catechol-rich hydrolysate. Cultivation was done at 30 °C, 250 rpm for 43 h. The data show mean values of triplicates with standard deviations.

To further increase MA titers, fed-batch strategies combining lignin hydrolysate and an additional carbon source have been shown to effectively maintain low hydrolysate concentrations while supporting higher product formation. Becker et al. (2018) demonstrated this strategy with *C. glutamicum*, achieving 12.5 mM (1.8 g L^{-1}) MA by feeding of catechol-rich hydrolysate and glucose using feed pulses containing approximately 1 mM catechol. Remarkably, an engineered *P. putida* reached 91.5 mM (13 g L^{-1}) MA within 54 h from HTC-processed lignin containing mainly catechol and phenol (Kohlstedt et al., 2018). To date, the only published example of MA production from a complex hydrolysate by a eukaryotic host involves *S. cerevisiae*, where Liu et al. (2020) reported co-production of 0.38 mM MA and ethanol from oil palm empty fruit bunch hydrolysate containing glucose and xylose.

These findings highlight the exceptional potential of *A. pullulans* as a promising eukaryotic production host, enabling a fully sustainable process that uses a lignin-derived hydrolysate and hemicellulose-derived sugars for producing value-added chemicals such as MA.

4. Conclusion

This study highlights the biotechnological potential of *A. pullulans* for valorizing lignin-derived aromatics. The strain demonstrated growth on diverse lignin monomers across a wide range of pH values, as well as on aromatic mixtures produced through lignin depolymerization. These results highlight its robustness and metabolic flexibility, which are essential traits for future industrial application. Deletion of *CATB* enabled efficient transformation of the lignin-derived monomer catechol into muconic acid. Scaling from microtiter plates to the bioreactor scale and implementing fed-batch mode increased the muconic acid titer to

23 g L^{-1}. The ability to utilize lignin hydrolysate together with xylose further demonstrates the suitability of *A. pullulans* for the utilization of complex feedstocks. Collectively, these findings position *A. pullulans* as a promising eukaryotic platform for sustainable lignin valorization. Looking forward, targeted metabolic engineering, process intensification, and exploration of additional products from lignocellulosic feedstocks represent key opportunities to further enhance its industrial relevance.

5. Declaration of generative AI and AI-assisted technologies in the manuscript preparation process

During the preparation of this work, the authors used ChatGPT to improve language and readability. After using this tool, the authors reviewed and edited the content as needed and take full responsibility for the content of the published article.

CRediT authorship contribution statement

Marielle Driller: Writing – review & editing, Writing – original draft, Visualization, Validation, Methodology, Investigation, Formal analysis, Data curation, Conceptualization. **Marius Grad:** Writing – review & editing, Writing – original draft, Methodology, Investigation, Data curation. **Marie Dielentheis-Frenken:** Writing – review & editing, Methodology, Investigation. **Karla Stein:** Writing – review & editing, Methodology. **Michael Kohlstedt:** Writing – review & editing, Writing – original draft, Supervision, Methodology, Investigation. **Christoph Wittmann:** Writing – review & editing, Supervision, Funding acquisition. **Lars M. Blank:** Writing – review & editing, Supervision, Funding acquisition. **Till Tiso:** Writing – review & editing, Supervision, Funding acquisition, Conceptualization, Methodology.

Declaration of competing interest

The authors declare that they have no known competing financial interests or personal relationships that could have appeared to influence the work reported in this paper.

Acknowledgements

The authors thank team Aureo for their support (Frederick Haala, Philipp Kohl, and Difan Xiao). Furthermore, the authors thank Tobias Karmainski for his support during fermentation and Carina Michel for her support with the TOM devices and during fermentation. The authors acknowledge the support of Adrian Gleissner during lignin depolymerization. The authors thank the German Federal Ministry of Education and Research (BMBF) for funding within the project *AureoFACTory* (no. 031B1203) and the Fachagentur Nachwachsende Rohstoffe (FNR) of the German Federal Ministry of Food and Agriculture (BMEL) within the project *ViRIDi Aurum* (no. 2220NR262X). Christoph Wittmann acknowledges support from the German Federal Ministry of Education and Research (BMBF) through grant STRAW2HEALTH (no. 031B1570). Michael Kohlstedt acknowledges support through a young investigator award sponsored by the Hans-and-Ruth-Giessen Foundation, St. Ingbert, Germany.

Appendix A. Supplementary data

Supplementary data to this article can be found online at https://doi.org/10.1016/j.biortech.2025.133851.

Data availability

Data will be made available on request.

References

Abdelaziz, O.Y., Brink, D.P., Prothmann, J., Ravi, K., Sun, M., García-Hidalgo, J., Sandahl, M., Hulteberg, C.P., Turner, C., Lidén, G., Gorwa-Grauslund, M.F., 2016. Biological valorization of low molecular weight lignin. Biotechnol. Adv. 34, 1318–1346. https://doi.org/10.1016/j.biotechadv.2016.10.001.

Anderlei, T., Zang, W., Papaspyrou, M., Büchs, J., 2004. Online respiration activity measurement (OTR, CTR, RQ) in shake flasks. Biochem. Eng. J. 17, 187–194. https://doi.org/10.1016/s1369-703x(03)00181-5.

Takuma, A., Kenta, T., Naofumi, K., Yuichiro, O., Muneyoshi, Y., Masaya, N., Eiji, M., 2020. The Syringate O-Demethylase Gene of *Sphingobium* sp. Strain SYK-6 is Regulated by DesX, while Other Vanillate and Syringate Catabolism Genes are Regulated by DesR. Appl. Environ. Microbiol. 86, e01712. https://doi.org/10.1128/AEM.01712-20.

Barton, N., Horbal, L., Starck, S., Kohlstedt, M., Luzhetskyy, A., Wittmann, C., 2018. Enabling the valorization of guaiacol-based lignin: Integrated chemical and biochemical production of *cis,cis*-muconic acid using metabolically engineered *Amycolatopsis* sp ATCC 39116. Metab. Eng. 45, 200–210. https://doi.org/10.1016/j.ymben.2017.12.001.

Becker, J., Kuhl, M., Kohlstedt, M., Starck, S., Wittmann, C., 2018. Metabolic engineering of *Corynebacterium glutamicum* for the production of *cis, cis*-muconic acid from lignin. Microb. Cell Fact. 17, 115. https://doi.org/10.1186/s12934-018-0963-2.

Becker, J., Wittmann, C., 2019. A field of dreams: Lignin valorization into chemicals, materials, fuels, and health-care products. Biotechnol. Adv. 37, 107360. https://doi.org/10.1016/j.biotechadv.2019.02.016.

Beckham, G.T., Johnson, C.W., Karp, E.M., Salvachúa, D., Vardon, D.R., 2016. Opportunities and challenges in biological lignin valorization. Curr. Opin. Biotechnol. 42, 40–53. https://doi.org/10.1016/j.copbio.2016.02.030.

Blaga, A.C., Gal, D.G., Tucaliuc, A., 2023. Recent advances in Muconic Acid Extraction Process. Appl. Sci. 13. https://doi.org/10.3390/app132111691.

Bourbonnais, R., Paice, M.G., 1987. Oxidation and reduction of lignin-related aromatic compounds by *Aureobasidium pullulans*. Appl. Microbiol. Biotechnol. 26, 164–169.

Carraher, J.M., Pfennig, T., Rao, R.G., Shanks, B.H., Tessonnier, J.-P., 2017. *cis, cis*-Muconic acid isomerization and catalytic conversion to biobased cyclic-C_6 -1,4-diacid monomers. Green Chem. 19, 3042–3050. https://doi.org/10.1039/C7GC00658F.

Chen, Z., Wan, C., 2017. Non-sterile fermentations for the economical biochemical conversion of renewable feedstocks. Biotechnol. Lett 39, 1765–1777. https://doi.org/10.1007/s10529-017-2429-8.

Choi, S., Lee, H.N., Park, E., Lee, S.J., Kim, E.S., 2020. Recent advances in Microbial production of *cis, cis*-Muconic Acid. Biomolecules 10. https://doi.org/10.3390/biom10091238.

Dessbesell, L., Paleologou, M., Leitch, M., Pulkki, R., Xu, C., (Charles),, 2020. Global lignin supply overview and kraft lignin potential as an alternative for petroleum-based polymers. Renew. Sustain. Energy Rev. 123, 109768. https://doi.org/10.1016/j.rser.2020.109768.

Gopinath, V., Murali, A., Dhar, K.S., Nampoothiri, K.M., 2012. *Corynebacterium glutamicum* as a potent biocatalyst for the bioconversion of pentose sugars to value-added products. Appl. Microbiol. Biotechnol. 93, 95–106. https://doi.org/10.1007/s00253-011-3686-4.

Gu, H., Zhu, Y., Peng, Y., Liang, X., Liu, X., Shao, L., Xu, Y., Xu, Z., Liu, R., Li, J., 2019. Physiological mechanism of improved tolerance of *Saccharomyces cerevisiae* to lignin-derived phenolic acids in lignocellulosic ethanol fermentation by short-term adaptation. Biotechnol. Biofuels 12, 1–14.

Haala, F., Dielentheis-Frenken, M.R.E., Brandt, F.M., Karmainski, T., Blank, L.M., Tiso, T., 2024. DoE-based medium optimization for improved biosurfactant production with *Aureobasidium pullulans*. Front. Bioeng. Biotechnol. 12, 1379707. https://doi.org/10.3389/fbioe.2024.1379707.

Huang, L.-Z., Ma, M.-G., Ji, X.-X., Choi, S.-E., Si, C., 2021. Recent Developments and applications of Hemicellulose from Wheat Straw: a Review. Front. Bioeng. Biotechnol. 9–2021. https://doi.org/10.3389/fbioe.2021.690773.

Jiménez, J.I., Miñambres, B., García, J.L., Díaz, E., 2002. Genomic analysis of the aromatic catabolic pathways from *Pseudomonas putida* KT2440. Environ. Microbiol. 4, 824–841. https://doi.org/10.1046/j.1462-2920.2002.00370.x.

Khalil, I., Quintens, G., Junkers, T., Dusselier, M., 2020. Muconic acid isomers as platform chemicals and monomers in the biobased economy. Green Chem. 22, 1517–1541. https://doi.org/10.1039/C9GC04161C.

Kim, K.H., Jeong, K., Zhuang, J., Jeong, H.J., Kim, C.S., Koo, B., Yoo, C.G., 2021. Tandem conversion of lignin to catechols via demethylation and catalytic hydrogenolysis. Ind. Crop. Prod. 159, 113095. https://doi.org/10.1016/j.indcrop.2020.113095.

Kohlstedt, M., Starck, S., Barton, N., Stolzenberger, J., Selzer, M., Mehlmann, K., Schneider, R., Pleissner, D., Rinkel, J., Dickschat, J.S., Venus, J., van Duuren, B.J.H., J, Wittmann, C.,, 2018. From lignin to nylon: Cascaded chemical and biochemical conversion using metabolically engineered *Pseudomonas putida*. Metab. Eng. 47, 279–293. https://doi.org/10.1016/j.ymben.2018.03.003.

Ladner, T., Held, M., Flitsch, D., Beckers, M., Büchs, J., 2016. Quasi-continuous parallel online scattered light, fluorescence and dissolved oxygen tension measurement combined with monitoring of the oxygen transfer rate in each well of a shaken microtiter plate. Microb. Cell Factories 15, 206. https://doi.org/10.1186/s12934-016-0608-2.

Li, M., Chen, J., He, K., Su, C., Wu, Y., Tan, T., 2024. *Corynebacterium glutamicum* cell factory design for the efficient production of *cis, cis*-muconic acid. Metab. Eng. 82, 225–237. https://doi.org/10.1016/j.ymben.2024.02.005.

Liu, T., Peng, B., Huang, S., Geng, A., 2020. Recombinant xylose-fermenting yeast construction for the co-production of ethanol and *cis, cis*-muconic acid from

lignocellulosic biomass. Bioresour. Technol. Rep. 9, 100395. https://doi.org/10.1016/j.biteb.2020.100395.
Meijnen, J.-P., de Winde, J.H., Ruijssenaars, H.J., 2008. Engineering *Pseudomonas putida* S12 for efficient utilization of D-xylose and L-arabinose. Appl. Environ. Microbiol. 74, 5031–5037. https://doi.org/10.1128/AEM.00924-08.
Nafian, F., Gharavi, S., Soudi, M.R., 2016. Degenerate primers as biomarker for gene-targeted metagenomics of the catechol 1, 2-dioxygenase-encoding gene in microbial populations of petroleum-contaminated environments. Ann. Microbiol. 66, 1127–1136. https://doi.org/10.1007/s13213-016-1197-3.
Ndukwe, J.K., Aliyu, G.O., Onwosi, C.O., Chukwu, K.O., Ezugworie, F.N., 2020. Mechanisms of weak acid-induced stress tolerance in yeasts: prospects for improved bioethanol production from lignocellulosic biomass. Process Biochem. 90, 118–130. https://doi.org/10.1016/j.procbio.2019.11.009.
Ookawa, Z., Higuchi, Y., Fujita, M., Sonoki, T., Kamimura, N., Masai, E., 2025. Catabolic System of Syringic Acid, a Key Intermediate of Lignin-Derived Aromatic Compounds, via a Novel Linear Pathway in Pseudomonas sp. NGC7. J. Agric. Food Chem. 73, 18899–18913. https://doi.org/10.1021/acs.jafc.5c04544.
Patra, P., Das, M., Kundu, P., Ghosh, A., 2021. Recent advances in systems and synthetic biology approaches for developing novel cell-factories in non-conventional yeasts. Biotechnol. Adv. 47, 107695. https://doi.org/10.1016/j.biotechadv.2021.107695.
Priefert, H., Rabenhorst, J., Steinbüchel, A., 2001. Biotechnological production of vanillin. Appl. Microbiol. Biotechnol. 56, 296–314. https://doi.org/10.1007/s002530100687.
Ramírez-Morales, J.E., Czichowski, P., Besirlioglu, V., Regestein, L., Rabaey, K., Blank, L. M., Rosenbaum, M.A., 2021. Lignin Aromatics to PHA Polymers: Nitrogen and Oxygen are the Key Factors for *Pseudomonas*. ACS Sustain. Chem. Eng. 9, 10579–10590. https://doi.org/10.1021/acssuschemeng.1c02682.
Rodriguez, A., Salvachúa, D., Katahira, R., Black, B.A., Cleveland, N.S., Reed, M., Smith, H., Baidoo, E.E.K., Keasling, J.D., Simmons, B.A., Beckham, G.T., Gladden, J. M., 2017. Base-Catalyzed Depolymerization of Solid Lignin-Rich Streams Enables Microbial Conversion. ACS Sustain. Chem. Eng. 5, 8171–8180. https://doi.org/10.1021/acssuschemeng.7b01818.
Rosini, E., Molinari, F., Miani, D., Pollegioni, L., 2023. Lignin Valorization: production of High Value-added Compounds by Engineered Microorganisms. Catalysts 13, 555. https://doi.org/10.3390/catal13030555.
Salvachúa, D., Johnson, C.W., Singer, C.A., Rohrer, H., Peterson, D.J., Black, B.A., Knapp, A., Beckham, G.T., 2018. Bioprocess development for muconic acid production from aromatic compounds and lignin. Green Chem. 20, 5007–5019. https://doi.org/10.1039/C8GC02519C.
Schweigert, N., Zehnder, A.J., Eggen, R.I., 2001. Chemical properties of catechols and their molecular modes of toxic action in cells, from microorganisms to mammals: minireview. Environ. Microbiol. 3, 81–91. https://doi.org/10.1046/j.1462-2920.2001.00176.x.
Umashankar, P., Nygård, Y., 2024. Filamentous fungi as emerging cell factories for the production of aromatic compounds. Fungal Biol. Biotechnol. 11, 19. https://doi.org/10.1186/s40694-024-00188-z.
Van den Bosch, S., Koelewijn, S.-F., Renders, T., Van den Bossche, G., Vangeel, T., Schutyser, W., Sels, B.F., 2018. Catalytic Strategies Towards Lignin-Derived Chemicals. Top. Curr. Chem. 376. https://doi.org/10.1007/s41061-018-0214-3.
Wagh, M.S., S, S., Nath, P.C., Chakraborty, A., Amrit, R., Mishra, B., Mishra, A.K., Mohanta, Y.K.,, 2024. Valorisation of agro-industrial wastes: Circular bioeconomy and biorefinery process – a sustainable symphony. Process Saf. Environ. Prot. 183, 708–725. https://doi.org/10.1016/j.psep.2024.01.055.
Wang, G., Tavares, A., Schmitz, S., França, L., Almeida, H., Cavalheiro, J., Carolas, A., Øzmerih, S., Blank, L.M., Ferreira, B.S., Borodina, I., 2022. An integrated yeast-based process for *cis,cis*-muconic acid production. Biotechnol. Bioeng. 119, 376–387. https://doi.org/10.1002/bit.27992.
Wang, P., Jia, S.-L., Liu, G.-L., Chi, Z., Chi, Z.-M., 2022. *Aureobasidium* spp. and their applications in biotechnology. Process Biochem. 116, 72–83. https://doi.org/10.1016/j.procbio.2022.03.006.
Wani, S.M., Mir, S.A., Khanday, F.A., Masoodi, F.A., 2021. Advances in pullulan production from agro-based wastes by *Aureobasidium pullulans* and its applications. Innov. Food Sci. Emerg. Technol. 74, 102846. https://doi.org/10.1016/j.ifset.2021.102846.
Weiland, F., Barton, N., Kohlstedt, M., Becker, J., Wittmann, C., 2023. Systems metabolic engineering upgrades *Corynebacterium glutamicum* to high-efficiency *cis, cis*-muconic acid production from lignin-based aromatics. Metab. Eng. 75, 153–169. https://doi.org/10.1016/j.ymben.2022.12.005.
Weiland, F., Kohlstedt, M., Wittmann, C., 2022. Guiding stars to the field of dreams: Metabolically engineered pathways and microbial platforms for a sustainable lignin-based industry. Metab. Eng. 71, 13–41. https://doi.org/10.1016/j.ymben.2021.11.011.
Weiland, F., Seo, K., Janz, F., Grad, M., Geldmacher, L., Kohlstedt, M., Becker, J., Wittmann, C., 2025. Metabolic engineering of *Corynebacterium glutamicum* for increased cis, cis-muconate production from plant-derived p-hydroxycinnamates via deregulated pathway flux and increased CoA intermediate availability. Metab. Eng. https://doi.org/10.1016/j.ymben.2025.08.004.
Wolf, S., Bullard, R., Buonocore, J.J., Donley, N., Farrelly, T., Fleming, J., González, D.J. X., Oreskes, N., Ripple, W., Saha, R., Willis, M.D., 2025. Scientists' warning on fossil fuels. Oxford Open Clim. Change 5, kgaf011. https://doi.org/10.1093/oxfclm/kgaf011.
Xiao, D., Driller, M., Dielentheis-Frenken, M., Haala, F., Kohl, P., Stein, K., Blank, L.M., Tiso, T., 2024. Advances in *Aureobasidium* research: Paving the path to industrial utilization. J. Microbial. Biotechnol. 17, e14535. https://doi.org/10.1111/1751-7915.14535.
Xiao, D., Driller, M., Stein, K., Blank, L.M., Tiso, T., 2025. Genome mining the black-yeast *Aureobasidium pullulans* NRRL 62031 for biotechnological traits. BMC Genomics 26, 244. https://doi.org/10.1186/s12864-025-11395-2.
Zhang, B., Xie, X., Zhu, H., Niu, B., Liang, D., Chen, K., Sun, W., Shi, D., 2024. Solid-state fermentation by *S. cerevisiae* with high resistance to ferulic acid improves the physicochemical properties of wheat bran and quality of bran-rich chinese steamed bread. J. Food Sci. 89, 954–965. https://doi.org/10.1111/1750-3841.16930.
Zhang, Z., Lu, Y., Chi, Z., Liu, G.L., Jiang, H., Hu, Z., Chi, Z.M., 2019. Genome editing of different strains of *Aureobasidium melanogenum* using an efficient Cre/loxp site-specific recombination system. Fungal Biol. 123, 723–731. https://doi.org/10.1016/j.funbio.2019.06.001.